Nature manuscript 2008-09-09567

Supplementary Notes, Supplementary Figures and Legends, Supplementary Legend to Movie 1 and Supplementary Discussion

Supplementary Note 1. The mouse AIM2-targeting siRNAs are derived from the 3'-untranslated region of mouse mRNA, whereas the human AIM2-targeting siRNAs are derived from the open reading frame of human AIM2 mRNA (Supplementary Fig. 13). These siRNAs do not share any sequence similarity with each other, or with the sequences of other mRNAs including mRNA for IFI16, IFIX or MNDA proteins. Indeed, the AIM2-targeting siRNAs had no effect on the expression of endogenous IFI16, IFIX or MNDA proteins in THP-1 cells or on the overexpressed IFI16, IFIX or MNDA proteins in 293T cells (Supplementary Fig. 5a and b). Thus the dampening effect of the AIM2-targeting siRNAs on inflammasome activation by cytoplasmic DNA in human THP-1 cells and in mouse macrophages can only be attributed to a specific knockdown of AIM2 protein in these cells.

Supplementary Note 2. Consistent with previous observations [1], we found that DNA from different sources, but not the dsRNA analog poly I:C, can activate caspase-1 and IL-1β in mouse WT and Nalp3$^{-/-}$ macrophages and in THP-1 cells (Supplementary Fig. 14, and data not shown). These results indicate that the observed response is specific to DNA, and that AIM2 does not require specific DNA sequences for its activation.

Supplementary Note 3. Because purified ASC can self-oligomerize and activate caspase-1 when incubated *in vitro* at 37° C even in the absence of its activators [2], we were unable to use purified ASC to assay the activity of AIM2. To circumvent this shortfall, we engineered a reporter chimeric procaspase-1 molecule with an N-terminal PYD of ASC instead of its own CARD domain (Supplementary Fig. 15). The chimeric procaspase-1 (PYD-caspase-1) can now interact directly with AIM2 without the need of the adaptor ASC. This chimera can also interact with the oligomeric ASC pyroptosome through self-association of the PYD.

1. Muruve, D. A. et al. The inflammasome recognizes cytosolic microbial and host DNA and triggers an innate immune response. Nature 452, 103-7 (2008).
2. Fernandes-Alnemri, T. et al. The pyroptosome: a supramolecular assembly of ASC dimers mediating inflammatory cell death via caspase-1 activation. Cell Death Differ 14, 1590-604 (2007).

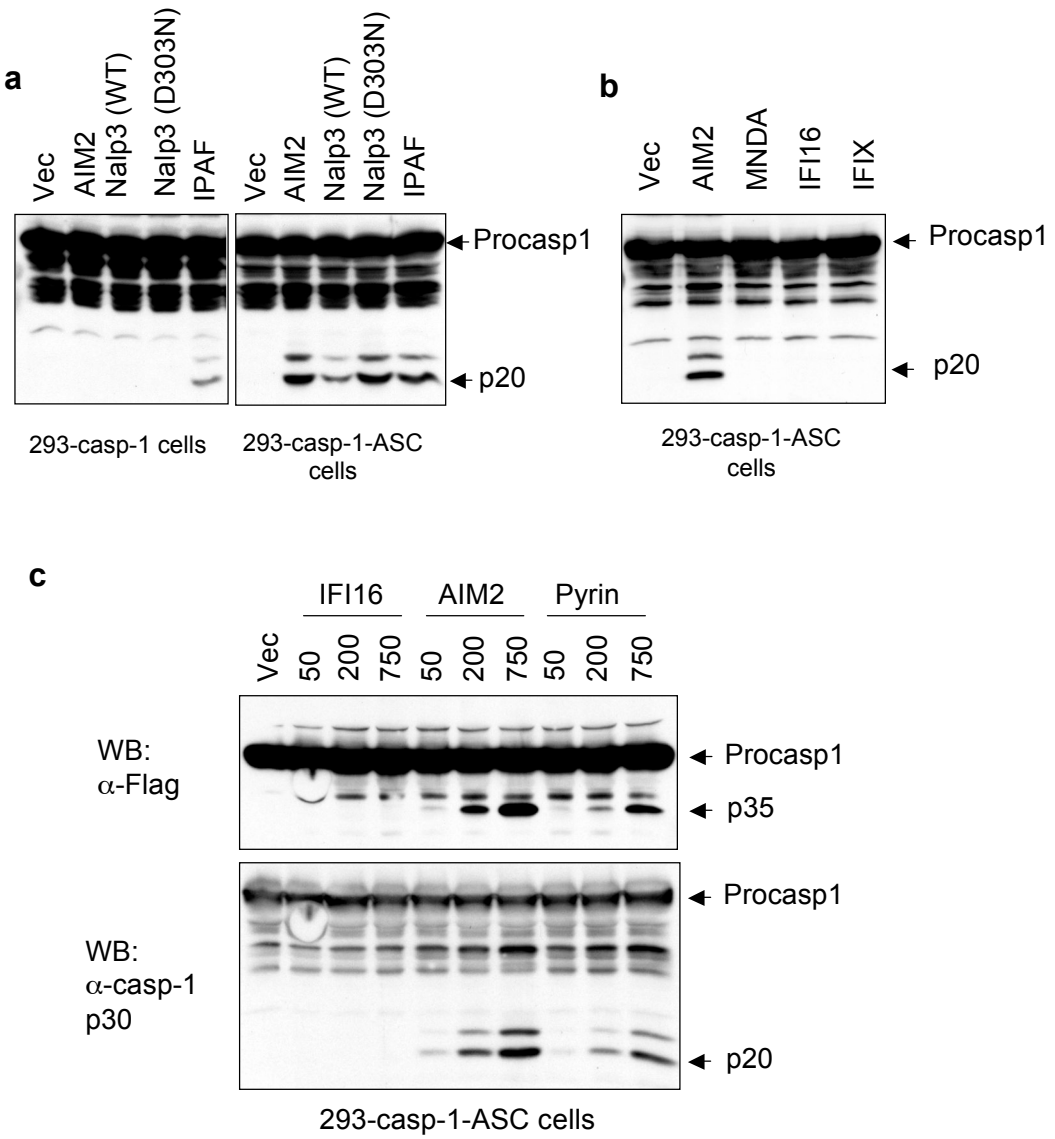

Supplementary Figure 1. Caspase-1 activation by AIM2 compared to other known activators of caspase-1 (pyrin, Nalp3 and Ipaf), and members of the human HIN-200 family (MNDA, IFI16 and IFIX). **a**, immunoblots for caspase-1 with anti-caspase-1 p30 antibody in cell lysates of 293-caspase-1 (left panel) and 293-caspase-1-ASC (right panel) cells transfected with empty vector (Vec), or the indicated expression plasmids for full-length AIM2, WT Nalp3, Nalp3-D303N mutant, or Ipaf (500 ng each plasmid). **b**, immunoblot for caspase-1 with anti-caspase-1 p30 antibody in cell lysates of 293-caspase-1-ASC cells transfected with empty vector (Vec), or the indicated expression plasmids for full-length AIM2, MNDA, IFI16, or IFIX (500 ng each plasmid). **c**, Immunoblots for caspase-1 with anti-Flag (upper panel) or anti-caspase-1 p30 (lower panel) antibody in cell lysates of 293-caspase-1-ASC cells (left panel) transfected with empty vector (Vec), or the indicated amounts (ng) of expression plasmids for full-length IFI16, AIM2, or pyrin.

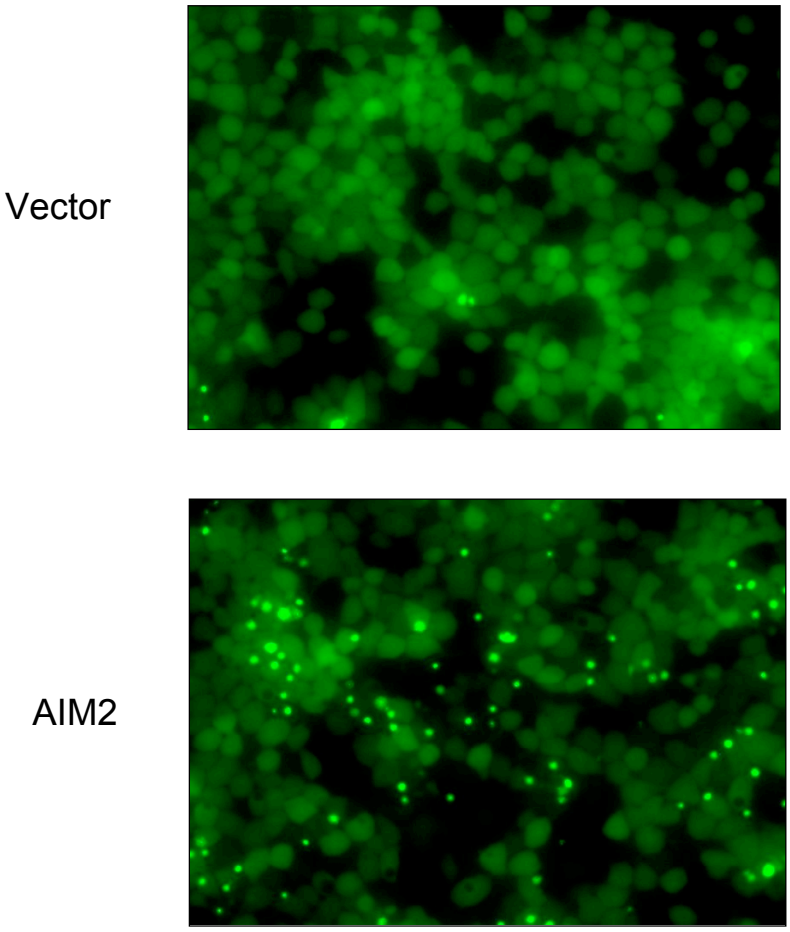

Supplementary Figure 2. ASC pyroptosome formation as visualized by fluorescence microscopy in stable 293-ASC-EGFP-N1 cells transfected with empty vector (*upper panel*) or an AIM2 expression construct (*lower panel*).

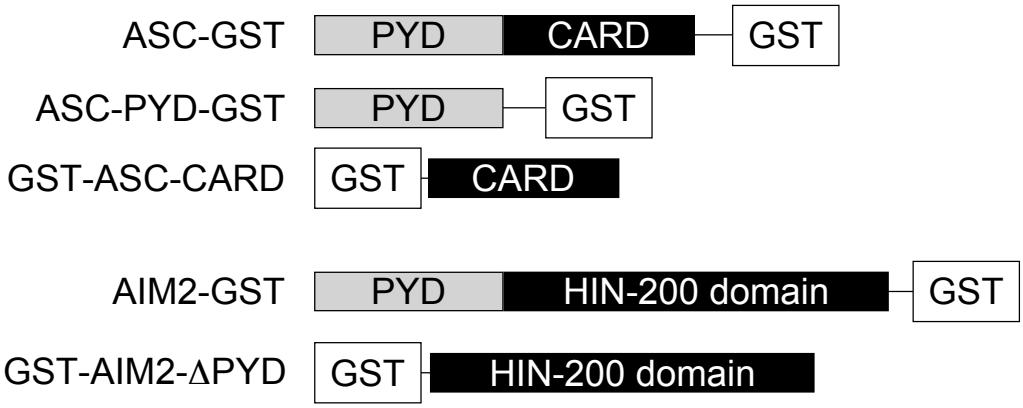

Supplementary Figure 3. Schematic diagrams showing the domain structure of ASC and AIM2, and their GST-fusion proteins used in the GST pull-down assays in Fig. 2a and b.

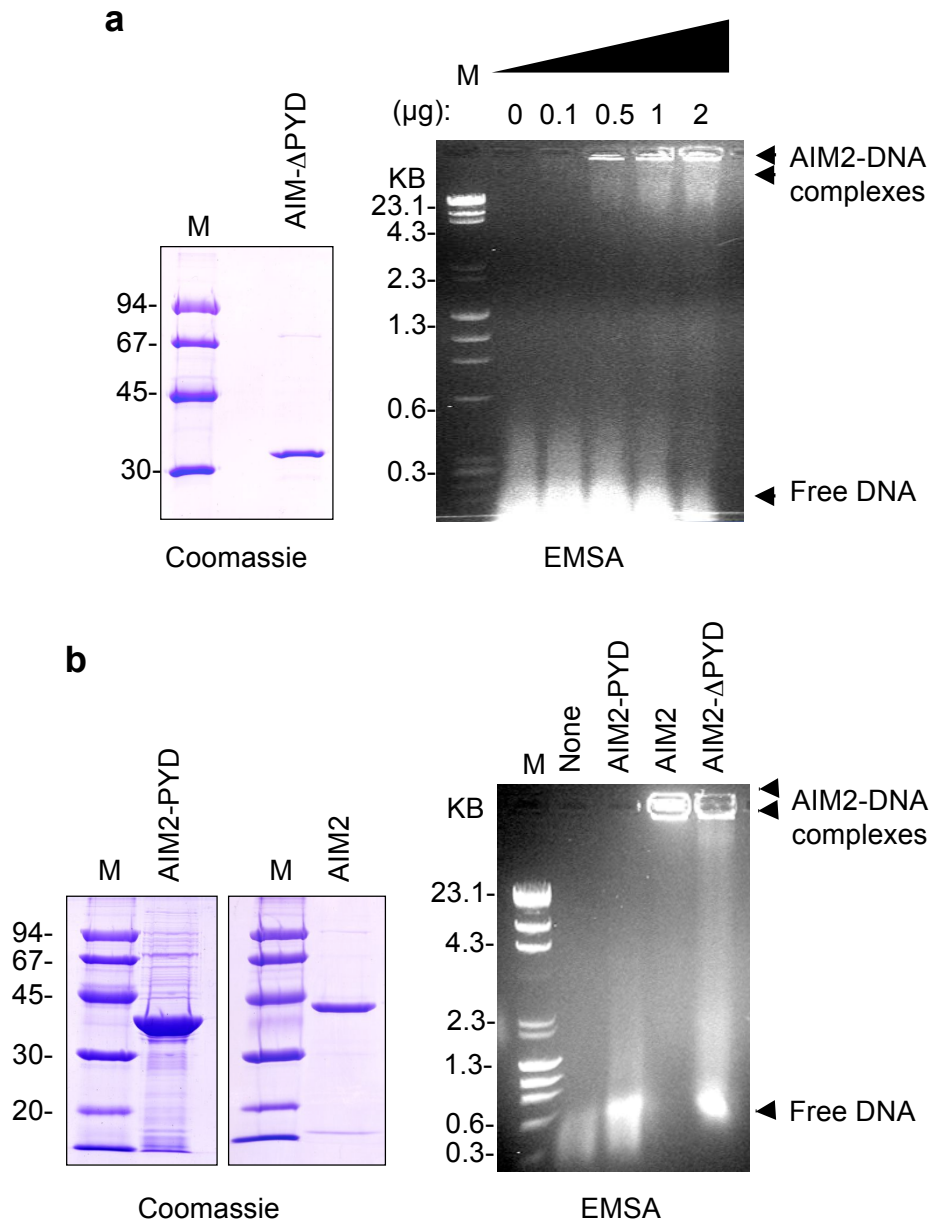

Supplementary Figure 4. EMSA of poly (dA:dT) DNA with full-length and truncated variants of AIM2. **a**, Right panel, ethidium bromide stained agarose gel showing EMSA with the indicated amounts of purified His6-tagged AIM2-ΔPYD and Poly (dA:dT) (2 μg). Left panel, a Coomassie stained gel of the affinity-purified AIM2-ΔPYD used in the EMSA. **b**, Right panel, ethidium bromide stained agarose gel showing the EMSA with 2 μg of purified PYD of AIM2 (3rd lane), full-length AIM2 (4th lane) or AIM2-ΔPYD (5th lane) and poly (dA:dT) (2 μg). Left panel, Coomassie stained gels of the affinity-purified GST-tagged PYD of AIM2 (PYD, left gel; 15 μg) and His6-tagged full-length AIM2 (AIM2, right gel, 2 μg), used in the EMSA. M, molecular weight markers.

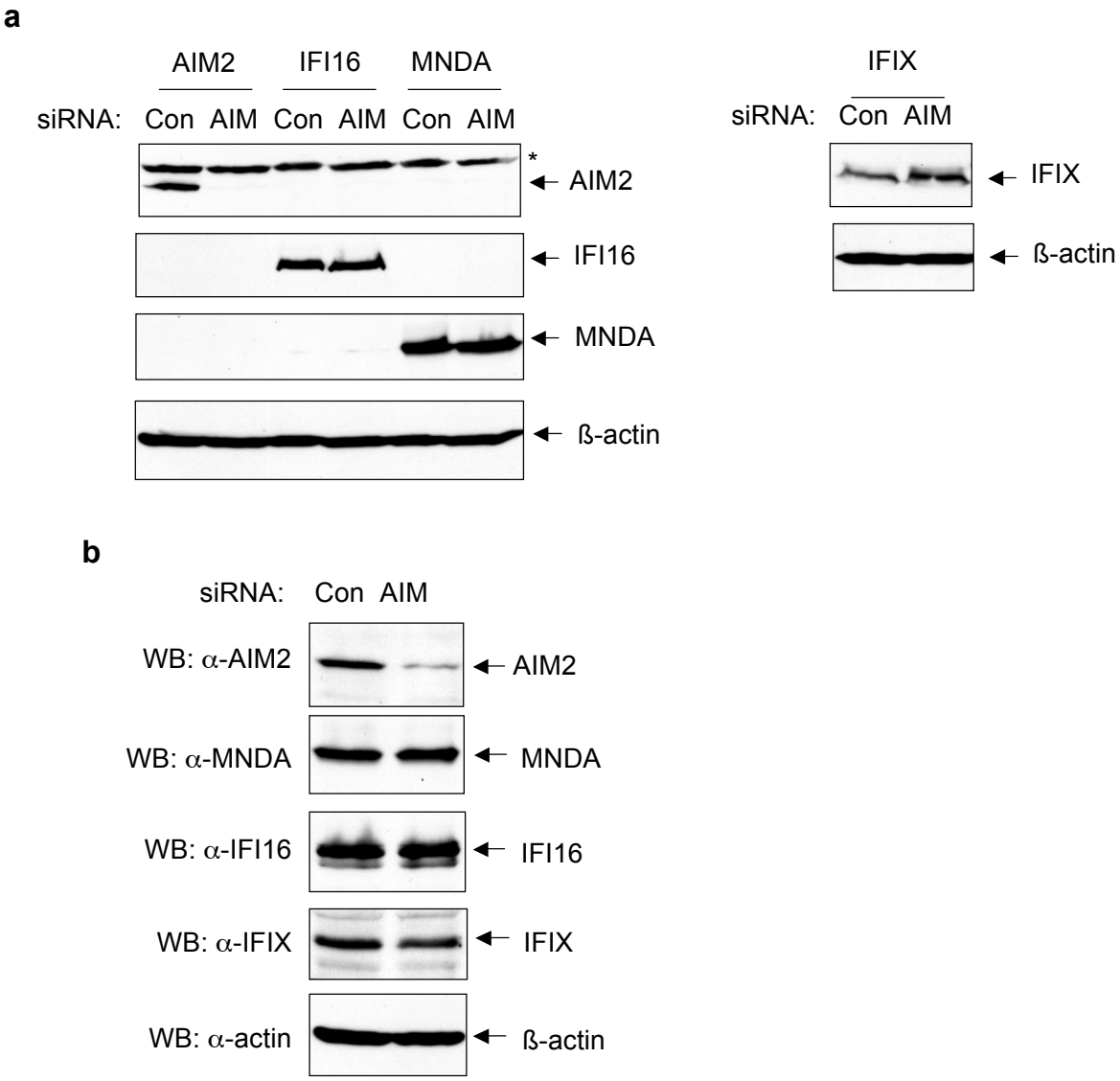

Supplementary Figure 5. Validation of the ability of the AIM2-targeting siRNA pool to specifically knockdown the expression of AIM2 protein in THP-1 and 293T cells. **a**, 293T cells (1 x 10^6 cells/well) in 35 mm 6-well plates were transfected with plasmids (0.5 μg/well) for full-length untagged human AIM2, IFI16, MNDA or IFIX cDNA, which contain the entire open-reading frames and the 5' and 3' untranslated regions of these genes together with non-targeting (con) or AIM2-targeting (AIM2) siRNA oligonuleotides (50 nM). 24 hours after transfection the expression of AIM2, IFI16, MNDA and IFIX were analyzed by immunoblot analysis with specific antibodies against AIM2 (Abnova), IFI16 (Santa Cruz), MNDA (Santa Cruz) or IFIX (a kind gift from Dr. Mien-Chie Hung). Notice the effective knockdown of the AIM2 protein with the AIM2-targeting siRNA and the absence of any effect on the expression of the other HIN-200 proteins. Asterisk indicate non-specific band. **b**, THP-1 cells were transfected with non-targeting (con) or AIM2-targeting (AIM2) siRNA oligonuleotides (50 nM). 24 hours after transfection cells were stimulated with interferon γ for 5 h and then total proteins from these cells were isolated and fractionated by SDS-PAGE followed by immunobloting with the indicated antibodies. Notice that AIM2-targeting siRNAs specifically reduce the expression of endogenous AIM2 protein but have no effect on the expression of IFI16, IFIX or MNDA proteins in THP-1 cells.

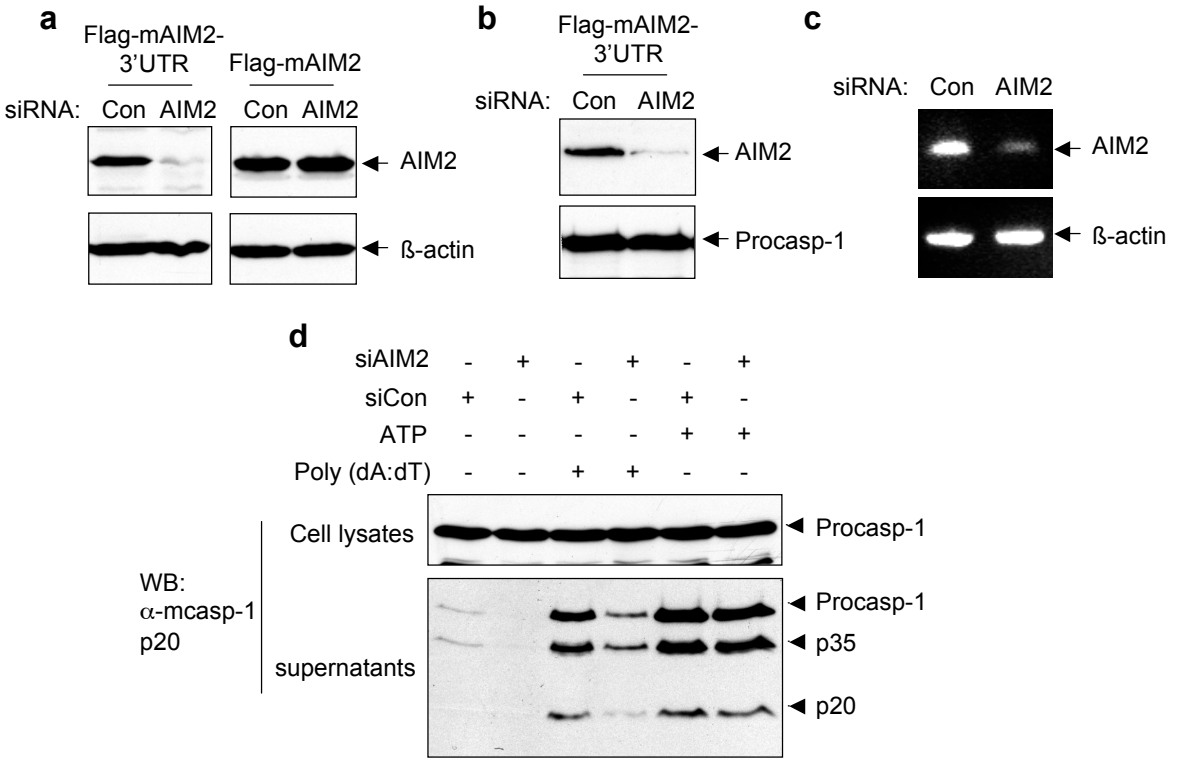

Supplementary Figure 6. **a**, **b**, **c**, Validation of the ability of the mouse AIM2-targeting siRNA pool to knockdown the expression of mouse AIM2 protein in 293T and ASC$^{-/-}$ macrophages. **a**, 293T (1 x 10^6 cells/well) cells in 35 mm 6-well plates were transfected with a Flag-tagged AIM2 expression plasmid (0.5 μg/well) that contains the full-length mouse AIM2 cDNA including the 3' untranslated region (3' UTR) (left panels), or a Flag-tagged AIM2 expression plasmid (0.5 μg/well) that contains the full-length mouse AIM2 cDNA without the 3' UTR (Flag-mAIM2, right panels) together with non-targeting (con) or mAIM2-targeting (AIM2) siRNA oligonuleotides (50 nM). 24 hours after transfection the expression of mAIM2 was analyzed by immunoblot analysis with an anti-Flag monoclonal antibody. Notice the significant knockdown of AIM2 (2nd lane, left panel) in the Flag-mAIM2-3'UTR-transfected cells, but not in the Flag-mAIM2-transfected cells, thus confirming the specificity of mAIM2 siRNAs which target the 3' UTR of mAIM2 mRNA. **b**, Immortalized ASC$^{-/-}$ macrophages were transfected with the Flag-mAIM2-3'UTR plasmid together with non-targeting (con) or mAIM2-targeting (AIM2) siRNA oligonuleotides. 24 hours after transfection the expression of mAIM2 was analyzed by immunoblot analysis with an anti-Flag monoclonal antibody. Notice the significant knockdown of AIM2 (2nd lane), indicating that the mAIM2-targeting siRNAs can efficiently knockdown AIM2 protein expression in mouse macrophages. ASC$^{-/-}$ macrophages were used in this experiment because they are resistant to plasmid DNA-induced cell death. The anti-Flag monoclonal antibody was used in these experiments because antibody against mouse AIM2 is currently unavailable. **c**, Nalp3$^{-/-}$ macrophages were transfected with non-targeting (con) or mAIM2-targeting (AIM2) siRNA oligonuleotides. 24 hours after transfection total RNA from these cells was reverse transcribed and subjected to 25 cycles of PCR with mAIM2 or β-actin specific oligonucleotides. The amplified cDNAs were analyzed on ethidium bromide-stained 1.5 % agarose gel. Notice the significant knockdown of endogenous mAIM2 mRNA by the mAIM2-targeting (AIM2) siRNAs. **d**, Immunoblot for mouse caspase-1 with an anti mouse p20 monoclonal antibody in culture supernatants of mouse WT bone marrow macrophages transfected with mouse AIM2-targeting siRNA (siAIM) or control non-specific siRNA (siCon) followed by transfection with or without poly (dA:dT), or treatment with LPS plus ATP as indicated.

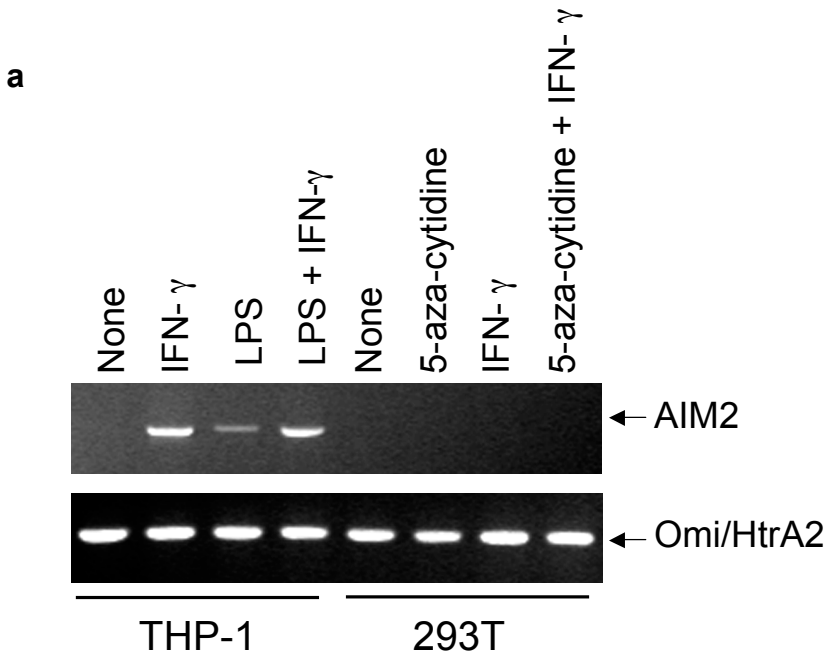

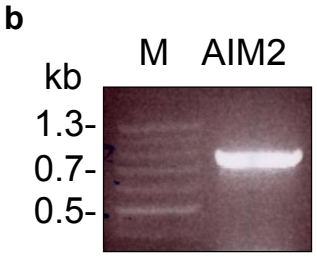

Supplementary Figure 7. Interferon gamma induces AIM2 in THP-1 macrophages but not in 293T cells. **a,** THP-1 macrophages (1st to 4th lanes) and 293T (5th to 8th lans) cells were treated with the indicated stimuli for 24h. Total RNA from these cells was reverse transcribed and subjected to 35 cycles of PCR with AIM2 specific oligonucleotides. The amplified cDNAs were analyzed on ethidium bromide-stained 1 % agarose gel. Notice the lack of effect of interferon gamma in the presence or absence of the DNA methyltransferase inhibitor 5-aza-cytidine on AIM2 expression in 293T cells, indicating that AIM2 gene is completely silenced in these cells. **b**, AIM2 is constitutively expressed in the v-*myc* and v-*raf* immortalized Nalp3$^{-/-}$ mouse macrophages. Total RNA from these cells was reverse transcribed and subjected to 35 cycles of PCR with mouse AIM2-specific oligonucleotides. The amplified AIM2 cDNA was analyzed on ethidium bromide-stained 1 % agarose gel.

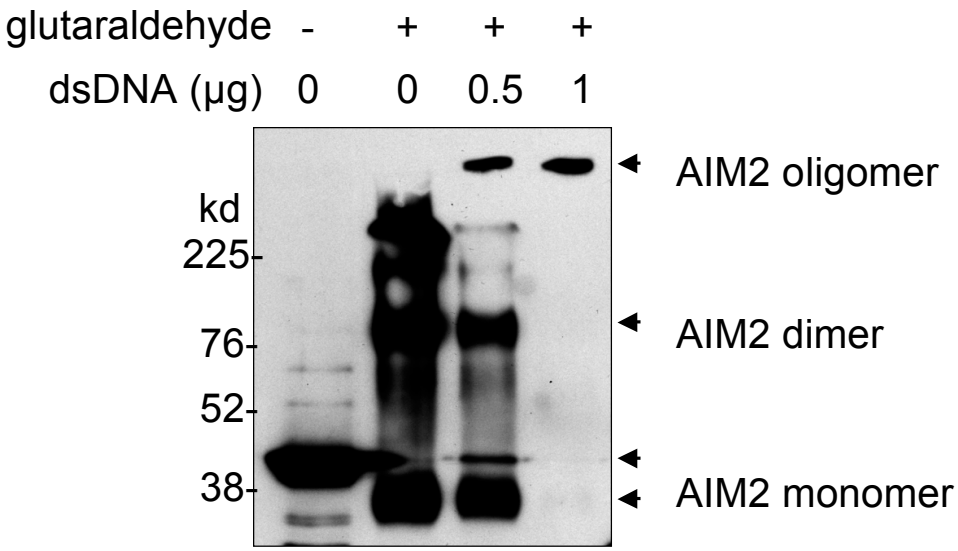

Supplementary Figure 8. Immunoblotting for AIM2 after cross-linking of purified AIM2 (2 μg) with glutaraldehyde in the presence of the indicated amounts of 64-mer dsDNA. This Figure shows a longer exposure of the same gel in Fig. 4d. Notice the complete conversion of the monomeric and dimeric AIM2 to the oligomeric form in the presence of 1 μg dsDNA (4^{th} lane).

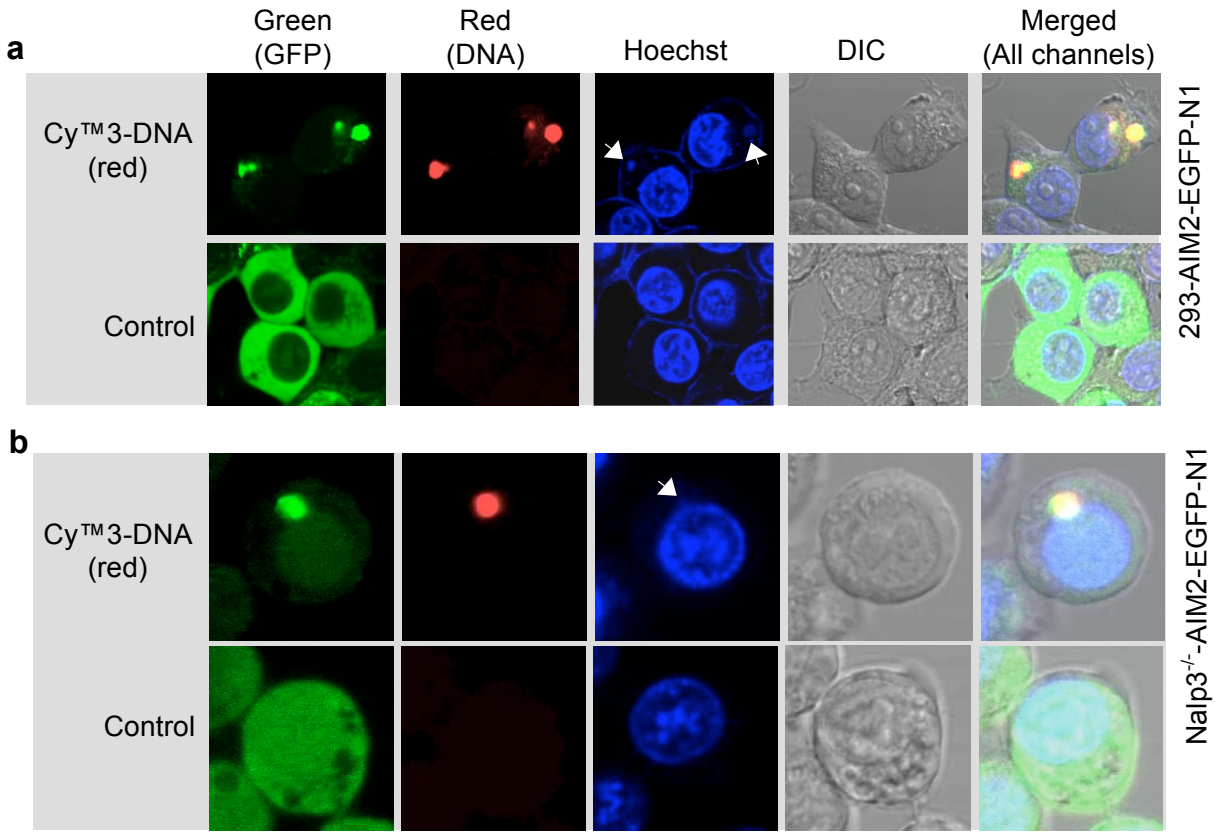

Supplementary Figure 9. Live cell imaging of cytoplasmic DNA-induced AIM2 oligomerization. Enlarged confocal live cell images of 293-AIM2-EGFP-N1 (**a**) or zVAD-FMK-pretreated Nalp3$^{-/-}$-AIM2-EGFP-N1 bone marrow macrophages (**b**) following transfection with Cy™3-labeled DNA (red, upper panels) or nothing (control, lower panels). The white arrows in the blue channels indicate staining of the cytoplasmic DNA with the blue Hoechst stain, which specifically stains DNA. Notice that zVAD-FMK prevents the pyroptotic cell death features induced by the Cy™3-labeled DNA in the Nalp3$^{-/-}$-AIM2-EGFP-N1 macrophages (**b**, upper panels).

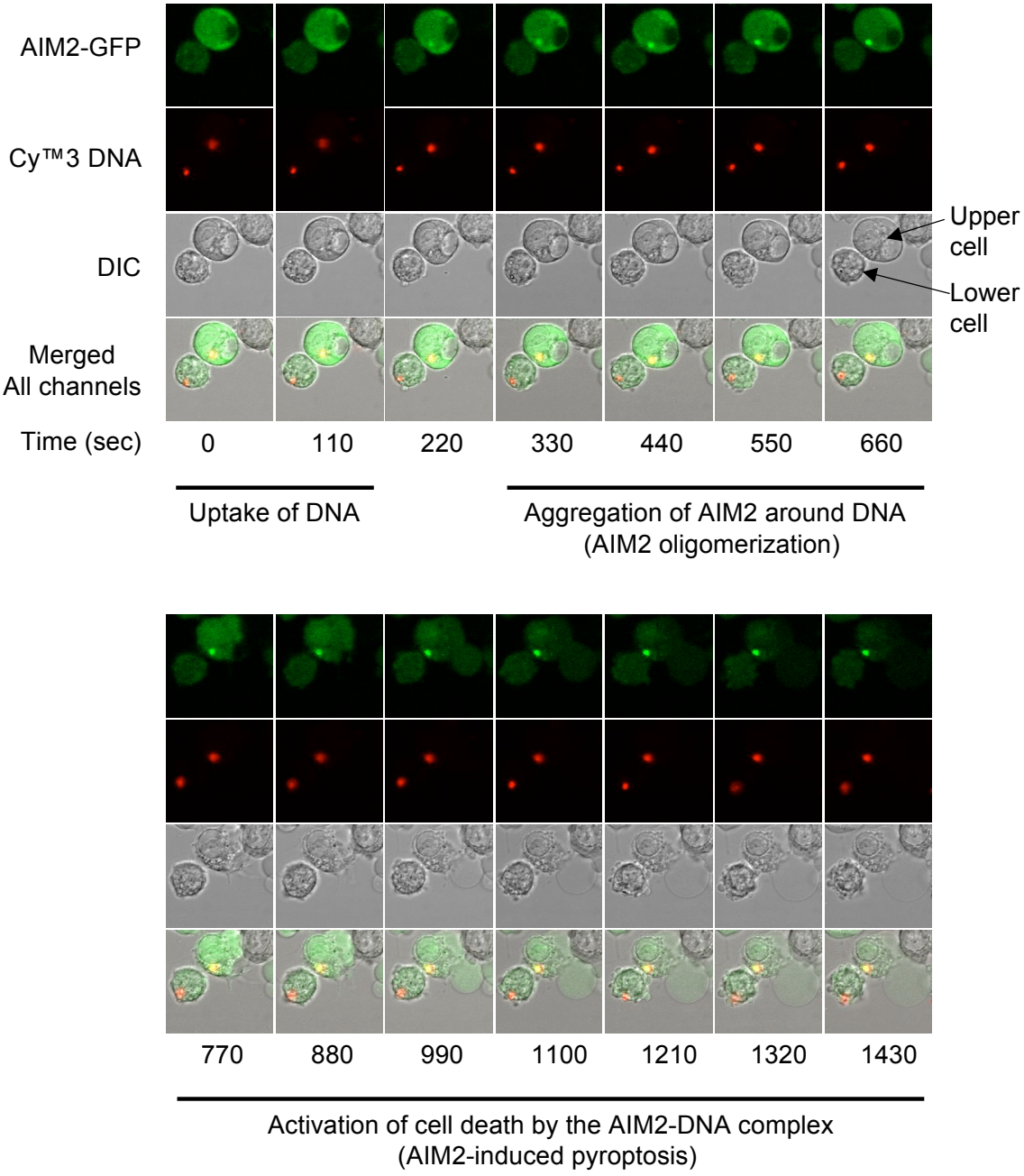

Supplementary Figure 10. Time-lapse live cell images of cytoplasmic DNA-induced AIM2 oligomerization and pyroptosis in Nalp3$^{-/-}$ bone marrow macrophages. Confocal live cell images of Nalp3$^{-/-}$-AIM2-EGFP-N1 bone marrow macrophages, which stably express a GFP-tagged AIM2, following transfection with Cy™3-labeled plasmid DNA. Images in the green (AIM2-GFP), red (Cy™3-DNA), and gray (DIC, Differential Interference Contrast) channels were recorded simultaneously every 22 sec. Selected images at 110 sec intervals are shown. Notice the uptake of DNA in the upper cell causes oligomerization of AIM2-GFP around the red DNA, which is followed by pyroptotic cell death with characteristic plasma membrane swelling. In the lower cell, DNA does not enter the cytoplasm and remains on the plasma membrane during this time, hence no pyroptosis is seen in this cell.

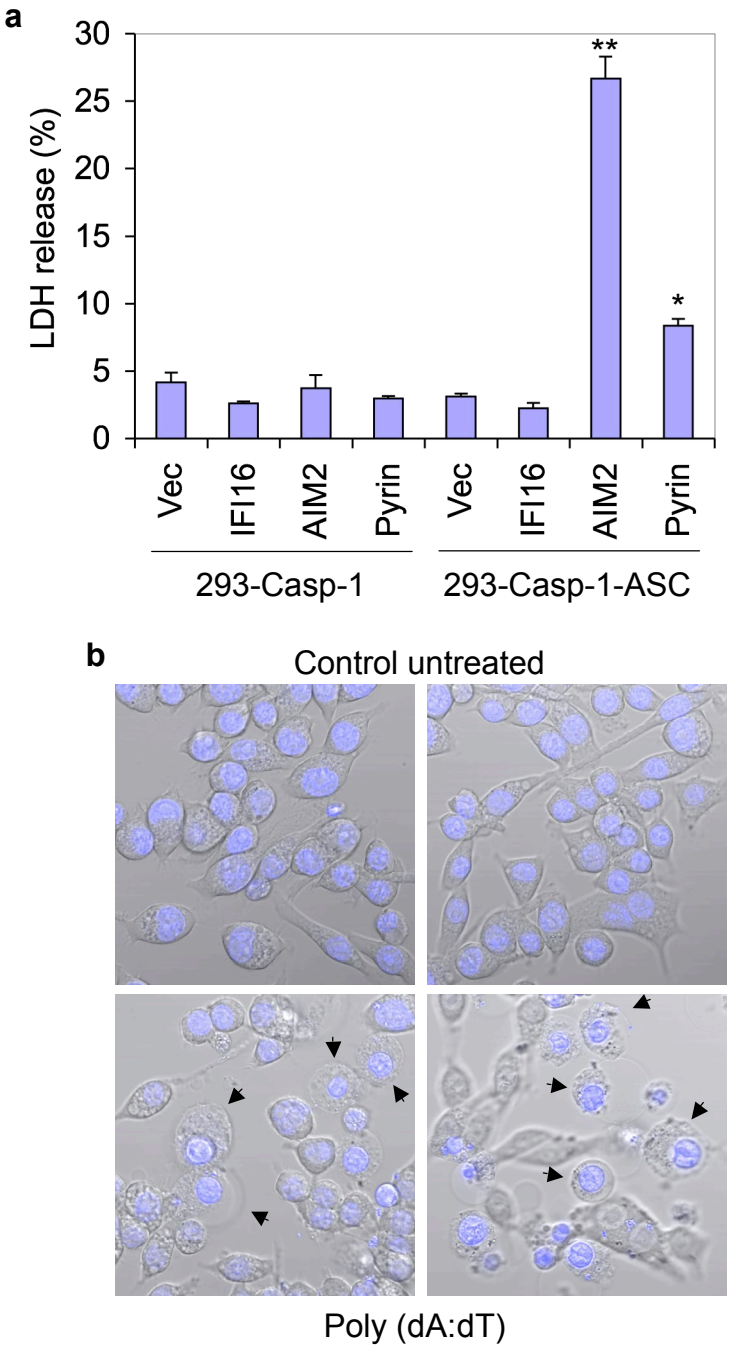

Supplementary Figure 11. Role of AIM2 in pyroptotic cell death. **a**, Percentages of LDH release into the culture medium of the indicated cell lines following transfection with the indicated plasmids (0.5 µg each/1 x 10^6 cells). Values represent mean ± S.D. (n = 3); *, P<0.01; **, P<0.005. **b**, Confocal live cell images showing pyroptotic cells (arrows) in poly (dA:dT)-transfected (bottom 2-panels) compared to vehicle-transfected control Nalp3$^{-/-}$ macrophages (top 2-panels). Two representative fields (40x magnification from the control and poly (dA:dT) cells are shown.

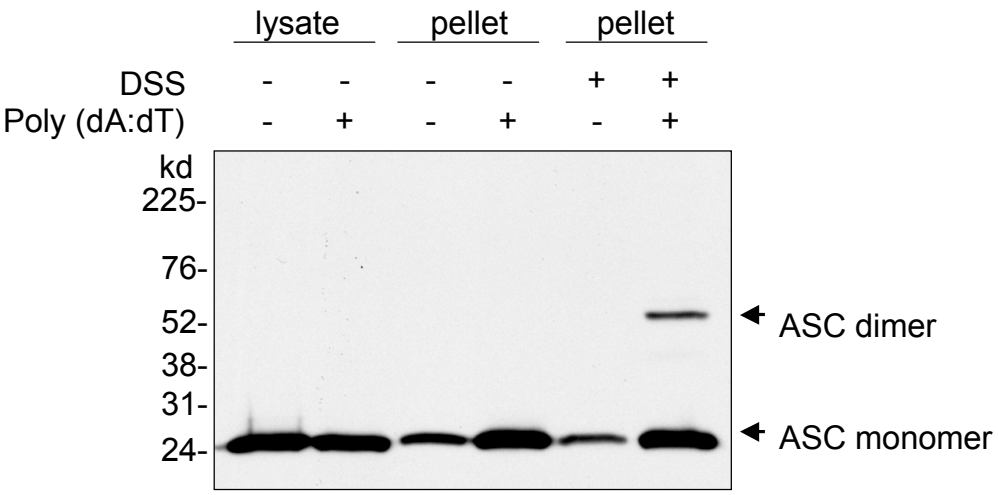

Supplementary Figure 12. Immunoblotting for poly (dA:dT)-induced pyroptosome formation in Nalp3-/- macrophages. This gel is a shorter exposure of the gel shown in Fig. 6b. Nalp3$^{-/-}$ macrophages were transfected with vehicle control (-) or poly (dA:dT) (+) for 4 h and then lysed. The endogenous ASC pyroptosomes present in the lysates (1st and 2nd lanes) were pelleted by centrifugation as described under 'Methods'. One-half of the pellets were cross-linked with DSS for 20 min (5th and 6th lanes) and the remaining one-half was left untreated (3rd and 4th lanes). The lysates and pellets were then fractionated by SDS-PAGE and Western blotted with anti-mouse ASC antibody. Notice the presence of the oligomeric ASC pyroptosome only in the pellets of the poly (dA:dT)-transfected macrophages (6th lane). The presence of small amounts of ASC in the pellets from the untreated cells is normal and is due to non-specific sedimentation of ASC with cellular debris. This form of ASC is non-oligomeric as evidence from the absence of oligomeric forms in the DSS-cross-linked sample (5th lane).

Supplementary Figure 13. Sequence alignment of the human (hAIM2) and mouse (mAIM2) cDNAs. The sequences of the human and mouse AIM2-targeting siRNAs used in this study are highlighted with yellow color and underlined. The open reading frame ATG is highlighted red, whereas the stop codons are highlighted blue. The sequences of the human and mouse AIM2-targeting siRNAs were found to have no significant sequence homology with HIN-200 family members or other known genes as determined by NCBI nBLAST program.

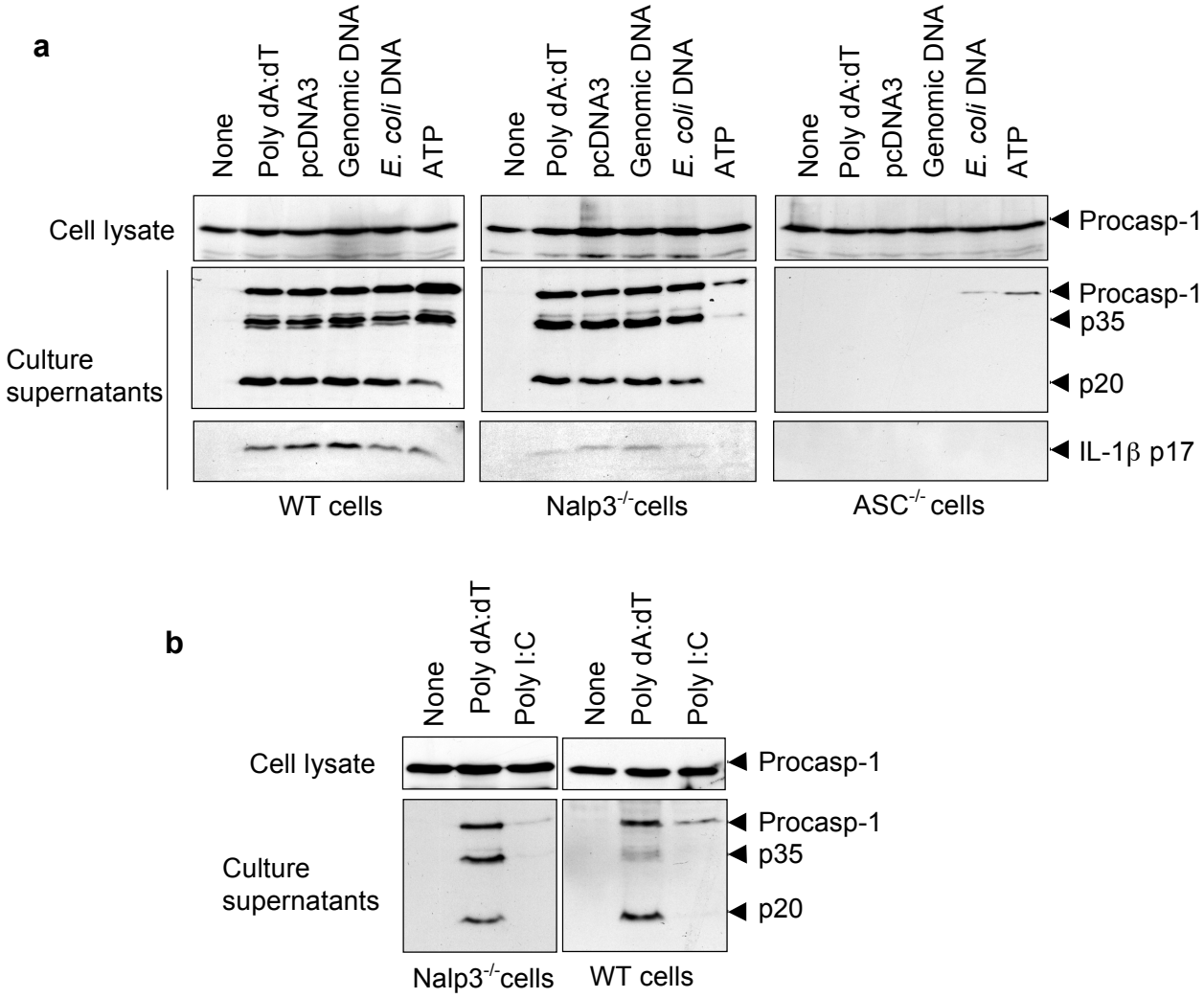

Supplementary Figure 14. DNA from different sources activates caspase-1 in mouse WT or Nalp3$^{-/-}$ but not in ASC$^{-/-}$ macrophages. **a**, Immunoblots for mouse caspase-1 (top and middle panels) and IL-1β p17 (lower panels) with anti-mcaspase-1-p20 or anti-IL-1β antibodies in cell lysates (top panels) and culture supernatants (middle and lower panels) of LPS-primed (1 μg/ml) WT, Nalp3$^{-/-}$ or ASC$^{-/-}$ macrophages transfected with nothing (none), poly (dA:dT), empty pcDNA plasmid, mouse genomic DNA or *E. coli* DNA or treated with ATP (5 mM) as indicated. Two μg of each plasmid DNA was used per 2 x10^6 cells. **b**, Same as above except that the indicated cells were transfected with poly (dA:dT) or poly I:C (2 μg).

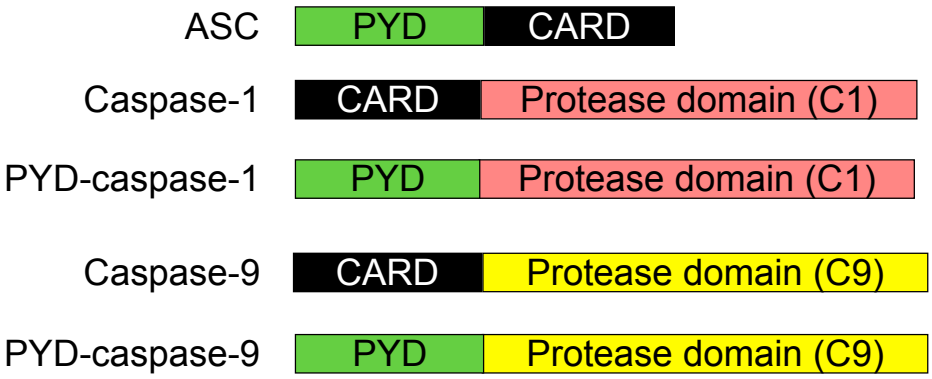

Supplementary Figure 15. Schematic diagrams showing the domain structures of ASC, procaspase-1 and procaspase-9, and the chimeric PYD-caspase-1 and PYD-caspase-9, which contain the PYD of ASC instead of their original CARD.

Supplementary Movie legend

Supplementary Movie 1. Time-lapse live cell movie of cytoplasmic DNA-induced AIM2 oligomerization and pyroptosis in Nalp3$^{-/-}$ bone marrow macrophages. Confocal live cell movie of Nalp3$^{-/-}$-AIM2-EGFP-N1 bone marrow macrophages, which stably express a GFP-tagged AIM2, following transfection with Cy™3-labeled plasmid DNA. Images in the green (AIM2-GFP), red (Cy™3-DNA), and gray (DIC, Differential Interference Contrast) channels were recorded simultaneously every 22 sec. Each channel shows a series of 75 images. Notice the uptake of DNA in the upper cell causes oligomerization of AIM2-GFP around the red DNA, which is followed by pyroptotic cell death with characteristic plasma membrane swelling. In the lower cell, DNA does not enter the cytoplasm and remains on the plasma membrane during this time, hence no pyroptosis is seen in this cell.

Supplementary Discussion

The identification of the AIM2 inflammasome as an important molecular platform capable of directly sensing cytoplasmic DNA and of triggering pro-inflammatory and cell death responses has important implications in human diseases. First, because AIM2 is an interferon inducible protein, viral and microbial pathogens that activate the interferon response are most likely sensed by the AIM2 inflammasome. For instance, cytosolic *Francisella tularensis* bacteria activate a Nalp3-independent, but ASC dependent inflammasome, that requires an intact type I interferon response for efficient inflammasome activation [1]. Inflammasome activation by *F. tularensis* also leads to cell death. Indeed, our preliminary results show that knocking down AIM2 in Nalp3$^{-/-}$ macrophages significantly reduced *F. tularensis*-induced caspase-1 activation (not shown). It is therefore likely that the AIM2 inflammasome participates in sensing *F. tularensis* infection and activation of caspase-1 and cell death in infected macrophages. The activation of this inflammasome thus represents a crucial innate immune response to pathogen-derived cytoplasmic DNA in general. Second, the AIM2 gene is located in a genetic locus that has been linked to the autoimmune disease systemic lupus erythematosus (SLE) [2]. In addition, AIM2 is one of a group of genes that is upregulated in Myasthenia gravis autoimmune disease [3]. Our data raises the possibility that the AIM2 inflammasome might be dysregulated in patients with active autoimmune diseases in general. Indeed, these diseases are associated with elevated levels of serum interferons and IL-1β [4, 5], most likely as a result of excess extracellular and cytoplasmic DNA that escapes from degradation and the activation of the AIM2 inflammasome. Finally, AIM2 is a putative tumor suppressor that was initially identified in a screen for suppressors of melanoma tumorigenicity [6]. Our data suggest that AIM2 is indeed a potential tumor suppressor that can kill cells in an ASC and caspase-1 dependent manner. The AIM2 pyroptotic pathway might not only be activated in response to

exogenously delivered cytoplasmic DNA, but perhaps could be activated in response to self DNA as a result of exposure to DNA damaging agents. Although a previous study showed that overexpressed AIM2 did not significantly alter the growth and survival of a number of melanoma cell lines in culture [7], this might be explained by the fact that ASC and caspase-1 are not expressed in many tumor cell lines. Indeed, the ASC and AIM2 genes are frequently silenced by DNA methylation, and frame shift and missense mutations in many tumors [8, 9], suggesting that inactivation of the AIM2 pyroptotic pathway might confer a growth advantage in these tumors. It will be of interest to see if certain DNA-damage induced tumors develop as a result of the inactivation of the AIM2 inflammasome. The discovery of the AIM2 inflammasome might therefore lead to new insights into the treatment of many nucleic-acid-dependent pathogenic and autoimmune diseases, and some forms of cancer.

1. Henry, T., Brotcke, A., Weiss, D. S., Thompson, L. J. & Monack, D. M. Type I interferon signaling is required for activation of the inflammasome during Francisella infection. J Exp Med 204, 987-94 (2007).
2. Choubey, D. & Panchanathan, R. Interferon-inducible Ifi200-family genes in systemic lupus erythematosus. Immunol Lett 119, 32-41 (2008).
3. Le Panse, R., Cizeron-Clairac, G., Bismuth, J. & Berrih-Aknin, S. Microarrays reveal distinct gene signatures in the thymus of seropositive and seronegative myasthenia gravis patients and the role of CC chemokine ligand 21 in thymic hyperplasia. J Immunol 177, 7868-79 (2006).
4. Crow, M. K. Type I interferon in systemic lupus erythematosus. Curr Top Microbiol Immunol 316, 359-86 (2007).
5. Sun, K. H., Yu, C. L., Tang, S. J. & Sun, G. H. Monoclonal anti-double-stranded DNA autoantibody stimulates the expression and release of IL-1beta, IL-6, IL-8, IL-10 and TNF-alpha from normal human mononuclear cells involving in the lupus pathogenesis. Immunology 99, 352-60 (2000).
6. DeYoung, K. L. et al. Cloning a novel member of the human interferon-inducible gene family associated with control of tumorigenicity in a model of human melanoma. Oncogene 15, 453-7 (1997).
7. Cresswell, K. S. et al. Biochemical and growth regulatory activities of the HIN-200 family member and putative tumor suppressor protein, AIM2. Biochem Biophys Res Commun 326, 417-24 (2005).
8. McConnell, B. B. & Vertino, P. M. TMS1/ASC: the cancer connection. Apoptosis 9, 5-18 (2004).
9. Woerner, S. M. et al. The putative tumor suppressor AIM2 is frequently affected by different genetic alterations in microsatellite unstable colon cancers. Genes Chromosomes Cancer 46, 1080-9 (2007).